Random Walks for Modelling Cell Populations
VRES 2013-14

Morgan Wall
n7532962

1 February 2014

1 Introduction

This report documents the tasks completed by Morgan Wall as part of his 2013-14 VRES scholarship with Dr. Matthew Simpson. The project covered the use of random walks in simulating cell motility, proliferation, and interaction in a variety of biological contexts. Furthermore, the derivation and analysis of partial differential equations to model equivalent processes was considered.

2 Simulating Random Walks in 2D

Random walk models are widely applicable to a variety of engineering contexts. Several models, either analsyed or proposed by Simpson, were researched [7, 8]. Each model accounted for cell motility and proliferation, which were essential to the various biological processes being considered. The models varied based on the consideration of cell interactions via volume exclusion or by the proliferation mechanism used. The models covered were reproduced using MATLAB and the C programming language in conjunction with Intel's Math Kernel Libraries (MKL).

2.1 Methodology

The methodology applied for simulating cell processes mimics that of Simpson's prior work [7, 8]. Simpson considered applying a rectangular lattice with nodes positioned equidistantly. As such, agents can assume positions at (i, j), where $i, j \in \mathbb{N}$. Each non-boundary node (i, j) therefore has the neighbouring nodes: $(i, j + 1)$, $(i, j - 1)$, $(i + 1, j)$, and $(i - 1, j)$. Random walk simulations are conducted on this lattice by intially placing agents at one or more nodes. Typically, a combination of periodic [2] and reflective boundary conditions [5] are imposed on the lattice.

For discrete cell simulations, random walks involve spatial and temporal parameters. Consequently, time must be discretised into a series of time steps. At the start of a time step, consider the case where there are N agents present. As per Simpson's approach, N agents are selected at random and each selection results in an agent being "updated".

Depending on the biological process being modelled, an "update" can include both motility and proliferation events. A motility event models cell movement and involves generating a random number from a uniform distribution in determining whether an agent attempts to move to an adjacent node. An adjacent node is consequently selected by generating another uniformly distributed random number S and...

2.2 Implementation

2.3 Results

In modelling a population of agents, Simpson derived partial differential equations by formulating an agent conservation statement for the average occupancy of a lattice site [8]. To demonstrate the reproduced model, simulations were conducted and compared against the following initial value problem (IVP):

$$\frac{\partial C}{\partial t} = D\frac{\partial^2 C}{\partial x^2} \qquad -\infty < x < \infty \tag{1}$$

$$C(x,0) = \begin{cases} 0 & x < -h \\ C_0 - h & -h < x < h \\ 0 & x > h \end{cases} \qquad -\infty < x < \infty \tag{2}$$

which has the analytic solution

$$C(x,t) = \frac{C_0}{2}\left(\operatorname{erf}\left(\frac{h-x}{2\sqrt{Dt}}\right) + \operatorname{erf}\left(\frac{h+x}{2\sqrt{Dt}}\right)\right). \tag{3}$$

This IVP was derived in [8] and is used to describe agent densities for a one-dimensional problem without proliferation. Density data was obtained from the reproduced model by performing simulations on a two-dimensional lattice with periodic boundary conditions and and averaging the occupancy of each column over multiple identically-prepared realisations. This IBVP was also solved numerically using a finite volume spatial discretisation with backward Euler time stepping. As seen in Figure 1, the reproduced model matches the analytic and numeric solutions closely as time elapses.

2.3.1 Additional Analysis

In exploring the various properties of the reproduced model, additional simulations were conducted for differing initial conditions and total realisations performed. As expected from (3), modifying the initial cell density merely scales the agent density curves (see Figure 2). Furthermore, as expected by the Law of Large Numbers, the accuracy of the reproduced model was dependent on the number of realisations averaged over [6]. As seen between Figures 1 and 3, an increase in the total realisations performed results in higher accuracy in the final solution.

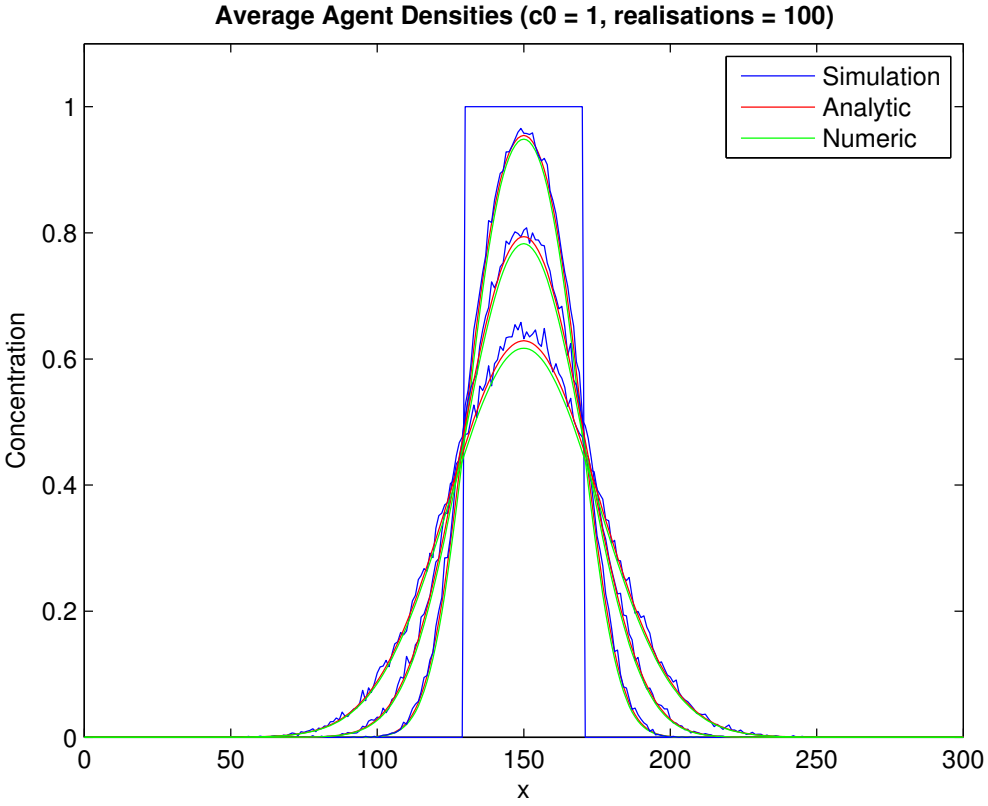

Figure 1: Comparison of agent density between the reproduced random walk model and the associated partial differential equation. Density data was obtained by averaging the occupancy of each column over 100 identically-prepared realisations satisfying (2) where $C_0 = 1$. Densities are given at $t = 0, 200, 500$, and 1000 and shows agent density diffusing across the lattice.

3 Random Lattices in 1D

In simulating cellular phenomena via random walk models, there exists three common methods for handling the spatial domain of interest: equally-spaced lattices, random lattices, and lattice free models. Lattices can be used under a variety of circumstances to discretise the spatial domain into a distinct set of nodes, which cells can consequently occupy. As discussed by Simpson [7], lattices can be constructed based off the expected size of a cell and the approximate distance they may move over a period of time. In constructing an equally-spaced lattice, nodes are spaced uniformly throughout a domain. Alternatively, nodes are positioned randomly or pseudorandomly within a domain in constructing a random lattice. Unfortunately, cells do not exhibit movement in a rigid, discrete manner, hence lattice-based models may not accurately simulate certain biological processes [3]. Lattice free models avoid this issue by not imposing a spatial discretisation on the simulations, which results in a major performance penalty.

Research was conducted into the application of random lattices in simulating cell motility in one dimension. Two approaches were taken in constructing a random lattice: perturbing

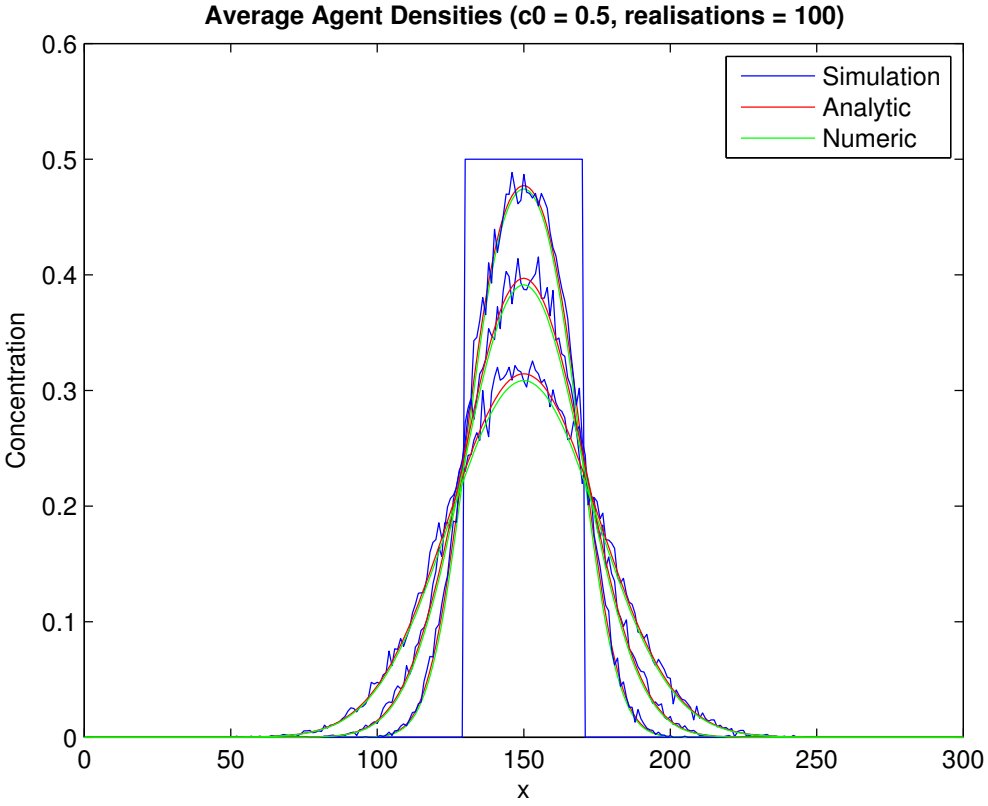

Figure 2: Comparison of agent density between the reproduced random walk model and the associated partial differential equation. Density data was obtained by averaging the occupancy of each column over 100 identically-prepared realisations satisfying (2) where $C_0 = 0.5$. Densities are given at $t = 0, 200, 500$, and 1000 and shows agent density diffusing across the lattice.

an equally-spaced lattice and generating node locations pseudorandomly. Let x_i be the position of the i^{th} node in the lattice. Under the perturbing approach, each node position is given by:

$$x_i = y_i + \Phi$$

where y_i is the location of the i^{th} unpertubed node in the equally-spaced lattice and Φ is a random variable. Additionally, let Δx be the fixed spacing between nodes on the equally-spaced lattice. Under the pseudorandom approach, each node position is given by:

$$x_i = \Theta$$

where Θ is a random variable. For all simulations, pseudorandom numbers were sourced from a variety of distributions using Intel's Vector Statistical Library (VSL).

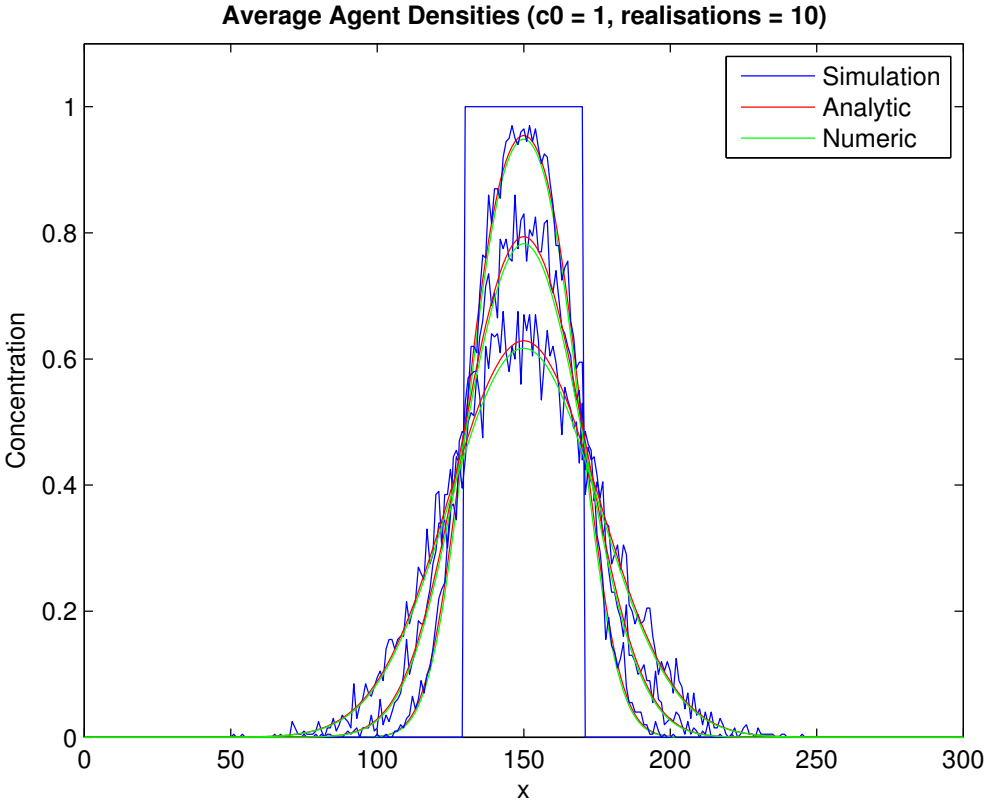

Figure 3: Comparison of agent density between the reproduced random walk model and the associated partial differential equation. Density data was obtained by averaging the occupancy of each column over 10 identically-prepared realisations satisfying (2) where $C_0 = 1$. Densities are given at $t = 0, 200, 500$, and 1000 and shows agent density diffusing across the lattice.

3.1 The Perturbing Approach

3.1.1 Lattice Properties

Initially, several key characteristics of lattices were identified in determining the preferred method for generating random lattices. The deltas between adjacent nodes and the existence of node clusters were of particular interest in generating physically realistic lattices for simulating cellular phenomenon. A series of random lattices were constructed on a dimensionless 1D region of 20 length units in which 20 nodes would be positioned. For the perturbation method, the equally-spaced lattice consisted of 20 nodes spaced one length unit apart with the first node residing at position zero.

Figure 4 depicts random lattices generated using the perturbation approach given by the continuous random variable

$$\Phi \sim \text{Uniform}(-\delta x, \delta x) \tag{4}$$

where δx is the maximum absolute perturbation allowed. These results quickly revealed that large perturbations are detrimental to the construction of random lattices since node

clustering is evident. For example, consider the lattices where $\delta x = 0.1$ and $\delta x = 0.5$. The former closely resembles an equally-spaced lattice whereas the latter exhibits node clustering around $x = 6$ and $x = 13$ and large unoccupied regions around $x = 5$. Such disparity in lattice spacing can result in erroneous simulations as cell motility can be subject to large variations in distance travelled per unit time. These findings are exacerbated as δx is increased further and is can be shown mathematically by considering the expected value and variance of the deltas between adjacent nodes.

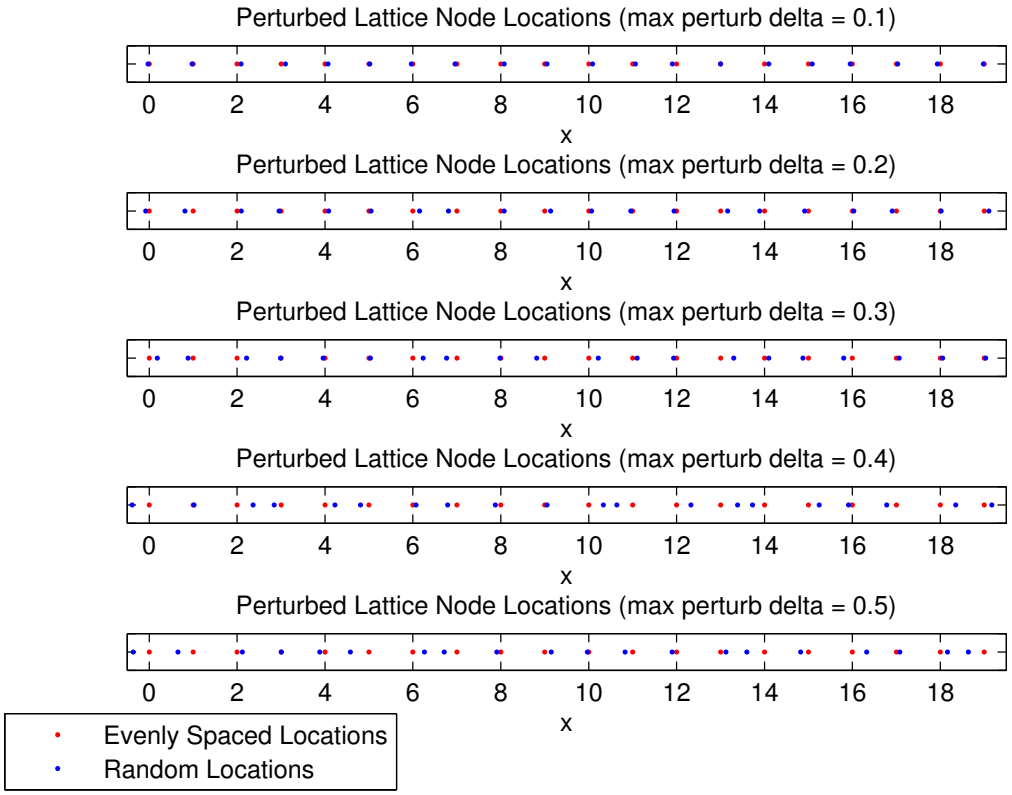

Figure 4: A series of randomly populated lattices generated by perturbing an equally-spaced lattice. Perturbations are sourced from a uniform distribution whose range is defined by a maximum allowable perturbation delta δx as given by (4). The investigated δx values range from 0.1 to 0.5.

Consider a random lattice generated using the perturbing approach and given the unperturbed lattice had a fixed node spacing Δx. Let A and B be independent and identically distributed random variables, then the expected node spacing is given by:

$$\begin{aligned} \mathrm{E}\left(x_i - x_{i-1}\right) &= \mathrm{E}\left(y_i + A - y_{i-1} - B\right) \\ &= \mathrm{E}\left(\Delta x + A - B\right) \\ &= \Delta x + \mathrm{E}\left(A\right) - \mathrm{E}\left(B\right) \\ &= \Delta x. \end{aligned}$$

As such, if we were to investigate the average delta between adjacent nodes over many meshes, for example, then by the Law of Large Numbers, the expected delta is that of

the equally-spaced lattice. This finding does not explicitly describe the existence of node clustering and large deltas between nodes as seen previously. Instead, consider finding the variance of the same statistic as follows:

$$\begin{aligned}
\mathrm{Var}\left(x_i - x_{i-1}\right) &= \mathrm{Var}\left(y_i + A - y_{i-1} - B\right) \\
&= \mathrm{Var}\left(\Delta x + A - B\right) \\
&= \mathrm{Var}\left(A - B\right) \\
&= \mathrm{Var}\left(A\right) + \mathrm{Var}\left(B\right) - 2\mathrm{Cov}\left(A, B\right) \\
&= \mathrm{Var}\left(A\right) + \mathrm{Var}\left(B\right) - 2\mathrm{E}\left(AB\right) + 2\mathrm{E}\left(A\right)\mathrm{E}\left(B\right) \\
&= 2\mathrm{Var}\left(A\right)
\end{aligned}$$

noting that $\mathrm{Var}\left(A\right) = \mathrm{Var}\left(B\right)$. Therefore the variability in the deltas between adjacent nodes is linearly proportional to the variance of the distribution from which perturbations are sourced from.

These same results were exhibited by averaging adjacent node spacings over a series of random lattices. For differing values of δx, 100 random lattices were generated in which 40 nodes were placed over a 1D region consisting of 40 dimensionless length units. As seen in Figure 5, the variability in minimum and maximum node spacings tends to increase linearly with δx. Furthermore, the mean node spacing (not shown) consistently converges to the expected value of $\Delta x = 1$ by the Law of Large Numbers. Additional analysis was conducted into the identification of node clustering in the absence of averaging, however, the results were somewhat inconclusive due to randomness and are not discussed here.

3.1.2 Simulating Random Walks

Random walks were conducted on perturbed lattices to obtain information regarding how such perturbations may impact cell motility. As per Simpson's analysis [8], the net agent displacement,

$$X_t - X_0 = \sum_{i=1}^{t} \left(X_i - X_{i-1}\right), \tag{5}$$

and the sum of squared displacements,

$$S_t = \sum_{i=1}^{t} \left(X_i - X_{i-1}\right)^2, \tag{6}$$

were investigated for different reasons. Note carefully the distinction between X_i and x_i: X_i is the location of a cell at the i^{th} time step whereas x_i is the location of the i^{th} node. The net displacement gives information on how a cell displaces itself from its starting position. Given the random walk method described section 2, it is expected that the net displacement should fluctuate about zero. On the other hand, the sum of square displacements is used to describe how the cell moves over the course of the simulation. As such, fluctuations can be observed as a cell travels over large distances and within node clusters, which is not adequately represented by (5). The expected sum of squared displacements is

$$\mathrm{E}\left(S_t\right) = \sum_{i=1}^{t} \mathrm{E}\left(\left(X_i - X_{i-1}\right)^2\right) \tag{7}$$

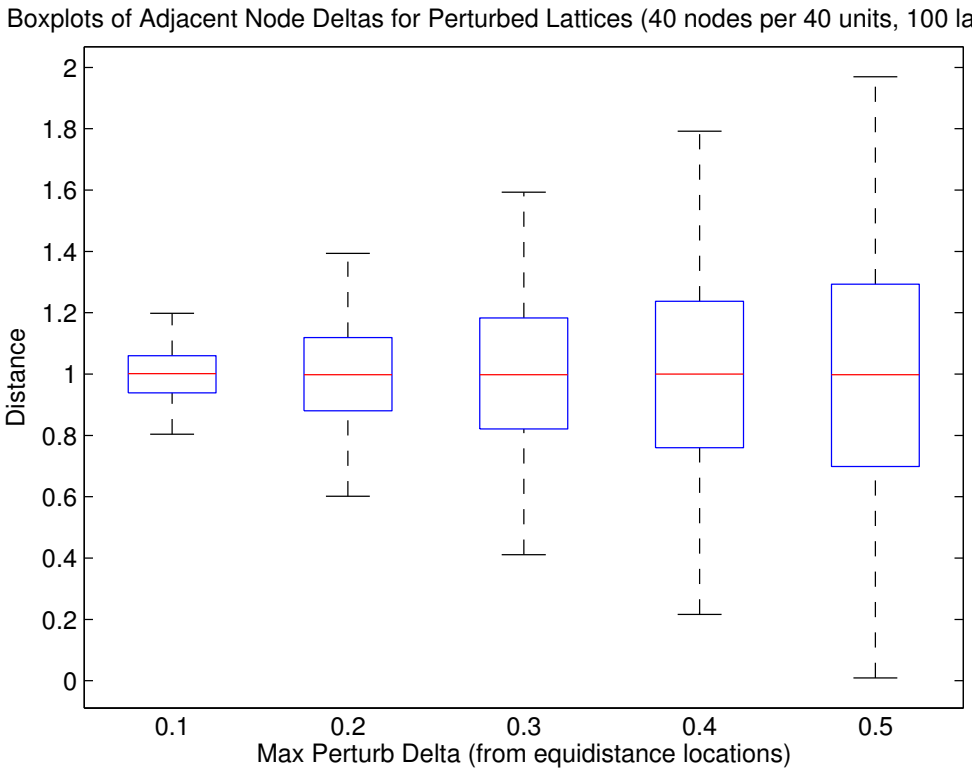

Figure 5: Boxplots of the spacing between adjacent nodes as collected over 100 random lattices for varying values of δx. Each random lattice consisted of 40 nodes spread over 40 dimensionless length units. The investigated δx values range from 0.1 to 0.5.

by the linearity of the expected value operator. Let A, B, and C be independent and identically distributed random variables and Δx be the spacing between nodes on the equally-spaced lattice. Additionally, suppose that at the i^{th} time step the cell is located at x_j. Now consider

$$\begin{aligned}
\mathrm{E}\left((X_i - X_{i-1})^2\right) &= \mathrm{E}\left(\frac{1}{2}(x_{j+1} - x_j)^2 + \frac{1}{2}(x_{j-1} - x_j)^2\right) \\
&= \frac{1}{2}\mathrm{E}\left((x_{j+1} - x_j)^2\right) + \frac{1}{2}\mathrm{E}\left((x_{j-1} - x_j)^2\right) \\
&= \frac{1}{2}\mathrm{E}\left((\Delta x + A - B)^2\right) + \frac{1}{2}\mathrm{E}\left((\Delta x + C - B)^2\right).
\end{aligned}$$

For brevity, consider

$$\begin{aligned}
\frac{1}{2}\mathrm{E}\left((\Delta x + A - B)^2\right) &= \frac{1}{2}\Delta x^2 + \Delta x \mathrm{E}(A - B) + \frac{1}{2}\mathrm{E}\left((A - B)^2\right) \\
&= \frac{1}{2}\Delta x^2 + \frac{1}{2}\left(\mathrm{E}\left(A^2\right) - 2\mathrm{E}(AB) + \mathrm{E}\left(B^2\right)\right).
\end{aligned}$$

Noting that A, B, and C and independent and $\mathrm{Var}(A) = \mathrm{Var}(B) = \mathrm{Var}(C)$,

$$\begin{aligned}\frac{1}{2}\mathrm{E}\left((\Delta x + A - B)^2\right) &= \frac{1}{2}\Delta x^2 + \frac{1}{2}\left(\mathrm{E}\left(A^2\right) - \mathrm{E}(A)^2 + \mathrm{E}\left(B^2\right) - \mathrm{E}(B)^2\right) \\ &= \frac{1}{2}\Delta x^2 + \frac{1}{2}\left(\mathrm{Var}(A) + \mathrm{Var}(B)\right) \\ &= \frac{1}{2}\Delta x^2 + \mathrm{Var}(B).\end{aligned}$$

Applying this result in simplifying (7), gives

$$\begin{aligned}\mathrm{E}\left((X_i - X_{i-1})^2\right) &= \frac{1}{2}\Delta x^2 + \mathrm{Var}(B) + \frac{1}{2}\Delta x^2 + \mathrm{Var}(B) \\ &= \Delta x^2 + 2\mathrm{Var}(B),\end{aligned}$$

therefore,

$$\mathrm{E}(S_t) = t\left(\Delta x^2 + 2\mathrm{Var}(B)\right). \tag{8}$$

Using a similar approach as above, in the absence of perturbation it can be shown that,

$$\mathrm{E}(S_t) = t\Delta x^2. \tag{9}$$

Alternatively, consider the case where there is no variance in the perturbations, which is equivalent to translating the domain of interest. In this case, (8) clearly reduces to (9). Therefore, as the variance in perturbations increases as does $\mathrm{E}(S_t)$.

Random walk simulations of a single agent (i.e. cell) were conducted over a series of lattices in ensuring the averaged results matched (8) and (9). Initially, equally-spaced lattices were considered for 500 time steps. Periodic boundary conditions were applied but never encountered by the agent by making the ratio of Δx and the length of the domain sufficiently small given the number of time steps. Linear least-squares fits were made to both the net displacement and the sum of squared displacements in comparing the results to the expected solutions. As seen in Figure 6, given that $\Delta x = 1$, the results match the expected solutions well with a fitted gradient for S_t of approximately 1.0.

As increasily large perturbations are introduced, the value of $\mathrm{E}(S_t)$ increased. For example, individual walks were conducted on 100 perturbed lattices where perturbations were sourced from (4) for $\delta x = 0.5$ and $\Delta x = 1$. As seen in Figure 7, the expected value of S_t has increased with δx compared to Figure 6. Under such a perturbation scheme, the expected gradient of S_t is

$$\mathrm{m} = \Delta x^2 + 2\mathrm{Var}(B) = 1 + \frac{1}{6} = \frac{7}{6} = 1.1\overline{6}.$$

The fitted gradients of 1.16 for S_t and 0.0 for $X_t - X_0$ match the expected values quite well. Similar results were produced for a variety of values for δx and are not discussed here.

The expected solutions derived earlier are general enough to apply to a variety of distributions. For example, perturbations were sourced from a Gaussian distribution with a mean of zero and a standard deviation of 0.2887. This standard deviation provides a variance equivalent to that of (4) with $\delta x = 0.5$, whose results are seen in Figure 7. Unsurprisingly, the same results are generated by sourcing from the Gaussian distribution as seen in Figure 8.

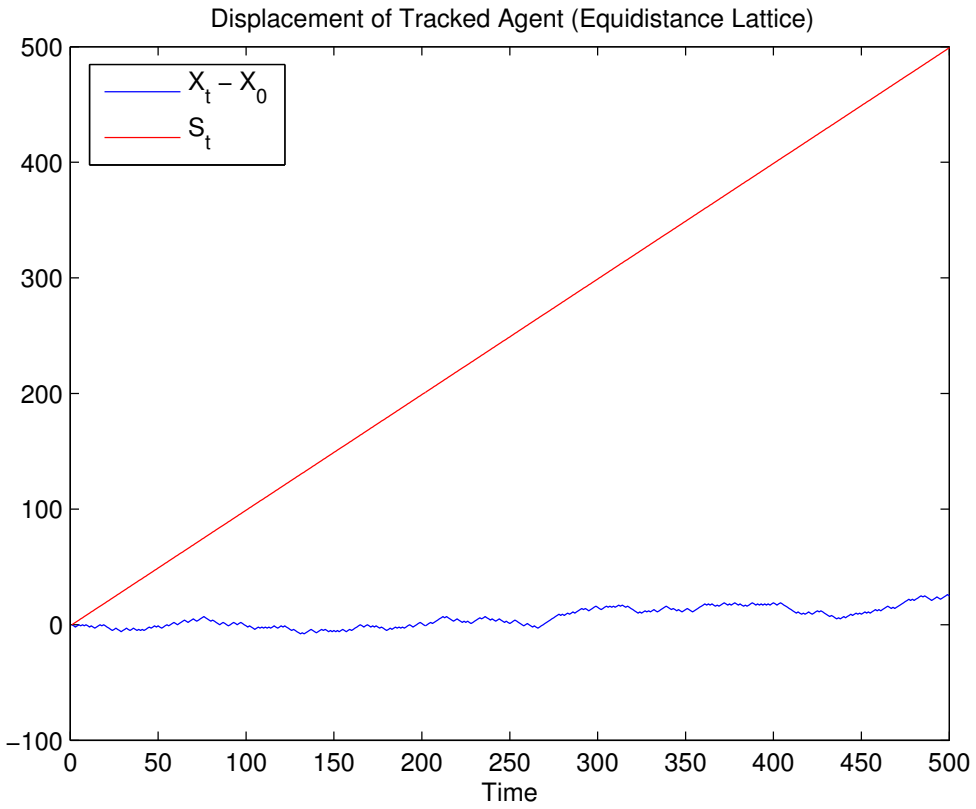

Figure 6: The progression of S_t and $X_t - X_0$ for a single agent over time on an equally-spaced lattice with $\Delta x = 1$. Linear least-squares fits were made from this data where the resultant functions were constrained to pass through $(0, 0)$. The fitted gradient for S_t was 1.0 and for $X_t - X_0$ it was 0.0 (rounded to one decimal place).

3.2 The Random Approach

3.2.1 Lattice Properties

As discussed in section 3.1.1, the deltas between adjacent nodes and the existance of node clusters was of particular interest in generating suitable lattices for simulating cellular phenomenon. Similar analysis was conducted in analysing both the random and perturbing approaches to allow comparison. As such, a series of random lattices were constructed on a dimensionless 1D region of 20 length units consisting of 20 nodes. Figure 9 depicts a series of random lattices generated by the random approach where

$$\Theta \sim \text{Uniform}\,(0, 20)\,. \tag{10}$$

In comparison to Figure 9, the random approach exhibits node clustering quite clearly. This is expected given that stochastic processes are more influential in deciding node positions in the random approach when compared to the perturbed approach. As such, the form of the random lattice will be dependent upon the distribution being sourced from. Therefore, any node clustering and large deltas between adjacent nodes can be avoided by sourcing a large number of node positions in creating a fine lattice.

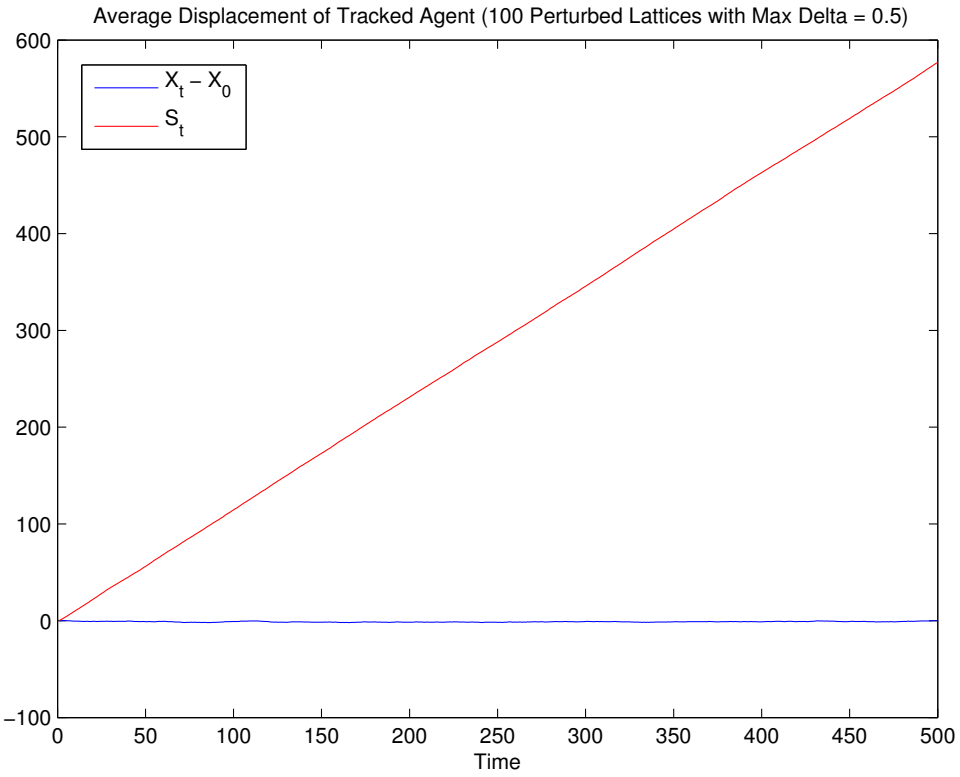

Figure 7: The progression of S_t and $X_t - X_0$ for a single agent over time averaged over 1000 perturbed lattices with $\Delta x = 1$ and perturbations sourced from (4). Linear least-squares fits were made from this data where the resultant functions were constrained to pass through $(0, 0)$. The fitted gradient for S_t was 1.16 and for $X_t - X_0$ it was 0.0 (rounded to two decimal places).

3.2.2 Simulating Random Walks

To compare with the perturbed method, random walks were conducted on lattices generated using the random approach. As such, the impact of the various generation methods could be further investigated. Using approaches similar to those applied in section 3.1.2, it can be shown that

$$\mathrm{E}\left(X_t - X_0\right) = 0$$

and

$$\mathrm{E}\left(S_t\right) = 2t\mathrm{Var}\left(\Theta\right)$$

where Θ is the random variable defining the locations the nodes. Several sets of simulations were designed and executed in an attempt to reproduce the expected results. Due to the large impact that stochastic processes have on this method it was computationally infeasible to construct simulations which would be impacted by the Law of Large Numbers. Either meshes would need to be extremely fine to compensate for the variability or a large number of simulations would need to be run. As such, generating random meshes using a purely pseudorandom method is arguably unsuitable for large scale simulations or applications which do not require a fine mesh.

Figure 8: The progression of S_t and $X_t - X_0$ for a single agent over time averaged over 1000 perturbed lattices with $\Delta x = 1$ and perturbations sourced from a Gaussian distribution with mean zero and a standard deviation of 0.2887. Linear least-squares fits were made from this data where the resultant functions were constrained to pass through $(0, 0)$. The fitted gradient for S_t was 1.16 and for $X_t - X_0$ it was 0.0 (rounded to two decimal places).

4 Investigating Travelling Wave Solutions

4.1 Phase Plane Analysis of Fisher's Equation

As part of modelling cell invasion fronts, travelling wave solutions of partial differential equations was researched. The travelling wave solutions of Fisher's equation for population growth,

$$\frac{\partial U}{\partial t} = \nu \frac{\partial^2 U}{\partial y^2} + kU(1 - U), \tag{11}$$

was thoroughly analysed via [1]. To ease subsequent analysis, (11) can be nondimensionalised via the unit-reducing substitutions:

$$\tau = \alpha t \qquad \text{and} \tag{12}$$

$$x = \beta y \tag{13}$$

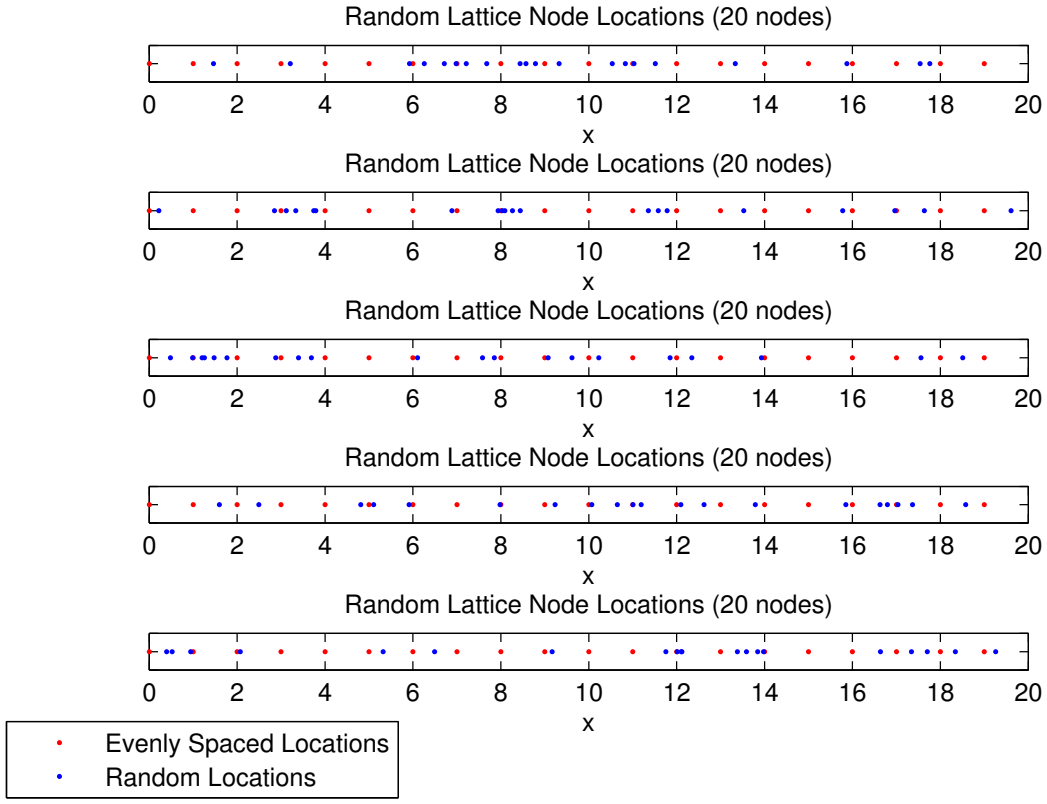

Figure 9: A series of randomly populated lattices generated by sourcing node positions from a uniform distribution spanning the region of interest as given by (10). Multiple lattices are displayed to illustrate the variability between lattices generated using this approach.

where α and β have units t^{-1} and m^{-1}, respectively. Applying the substitution in (12) and the chain rule, we obtain:

$$\frac{\partial U}{\partial \tau}\frac{d\tau}{dt} = \nu\frac{\partial^2 U}{\partial y^2} + kU(1-U)$$
$$\alpha\frac{\partial U}{\partial \tau} = \nu\frac{\partial^2 U}{\partial y^2} + kU(1-U)$$

By inspection, it is clear that (11) can be nondimensionalised in time and simplified when $\alpha = k$. Hence,

$$\frac{\partial U}{\partial \tau} = \frac{\nu}{k}\frac{\partial^2 U}{\partial y^2} + U(1-U) \tag{14}$$

Applying (13) in a similar manner gives

$$\frac{\partial U}{\partial \tau} = \frac{\beta^2\nu}{k}\frac{\partial^2 U}{\partial x^2} + U(1-U).$$

As such, (14) can be nondimensionalised in space and simplified when $\beta = \sqrt{k/\nu}$, which results in

$$\frac{\partial U}{\partial \tau} = \frac{\partial^2 U}{\partial x^2} + U(1-U). \tag{15}$$

As discussed by Canosa [1], this nondimensionalised equation describes nonlinear population growth in one spatial dimension. Consequently, the modelled habitat (i.e. space) can only feasibly support a maximum population per unit length. Given the form of the logistic source term in (15), suppose that maximum population is unity. The following initial condition can therefore be applied:

$$0 \leq U(x,0) \leq 1, \qquad -\infty < x < \infty. \tag{16}$$

Canosa [1] was specifically interested solving (15) subject to (16) such that all the derivatives in x tended to zero as $x \to \pm\infty$ coupled with the following far-field conditions:

$$\lim_{x\to-\infty} U(x,\tau) = 1 \qquad \lim_{x\to\infty} U(x,\tau) = 0 \qquad t \geq 0. \tag{17}$$

Any one-dimensional partial differential equations in space and time, $U(x,\tau)$, exhibiting travelling wave solutions supports the transformation

$$U(x,t) = U(x - c\tau) \equiv U(s) \tag{18}$$

which merges both time and space variables to provide a "standing wave" solution where the spatial origin is locked at the peak of the travelling wave moving at speed c. As such, the spatial coordinate system can be seen to translate in time in moving with the peak of the wave. Applying (18) with the chain rule gives

$$-c\frac{dU}{ds} = \frac{d^2U}{ds^2} + U(1-U)$$

which has reduced Fisher's equation into a second order non-linear partial differential equation. This equation can be further simplified into the following system of first order differential equations

$$\frac{dU}{ds} = V(s) \tag{19}$$

$$\frac{dV}{ds} = U^2 - U - cV. \tag{20}$$

Phase plane analysis was conducted on (19) and (20) using pplane8 for MATLAB [4].

Fisher originally discovered that (11) has travelling wave solutions where $c \geq 2$. This fact can be verified by solving the eigenvalue problem associated with (19) and (20) to determine the nature of any critical points in the phase plane. Given $c \geq 2$ it can be shown that, $(U,V) = (0,0)$ is a stable node and $(U,V) = (1,0)$ is a saddle point. Conversely, given $c < 2$, $(U,V) = (0,0)$ is a stable spiral. The phase planes seen in Figures 10 and 11 illustrate these results for specific values of c. Figure 10 exhibits the physically impossible solutions for $c < 2$ as discussed by Canosa [1]. Note how certain phase trajectories can lead to negative values of U, which is physically impractical in modelling population growth.

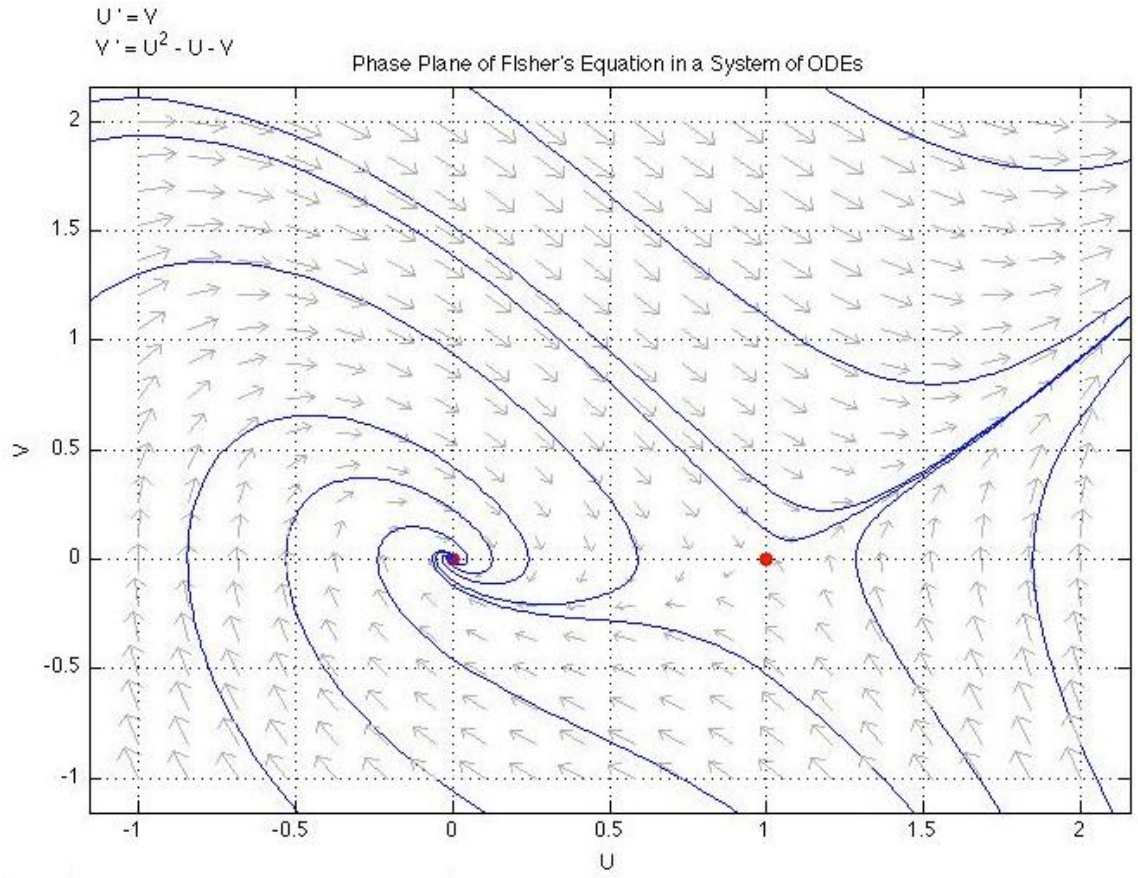

Figure 10: Phase plane of the system of ODEs that describe the travelling wave solutions to Fisher's equation, where $C = 1$. The red dots are the critical points and the blue lines are the phase trajectories. At $(0, 0)$ there is a spiral sink and at $(1, 0)$ there is a saddle point.

4.2 Solving Fisher's Equation

In order to better understand the travelling wave solutions to Fisher's equation, the following IBVP was solved numerically using MATLAB's pdepe function:

$$\begin{aligned}
\frac{\partial U}{\partial \tau} &= \frac{\partial^2 U}{\partial x^2} + U(1-U) && 0 \le x \le 100 && t \ge 0 \\
U(0,\tau) &= 1 && \tau \ge 0 \\
U(100,\tau) &= 0 && \tau \ge 0 \\
U(x,0) &= \begin{cases} 1 & x \le 50 \\ 0 & \text{otherwise} \end{cases} && 0 \le x \le 100.
\end{aligned}$$

The solutions, for varying timesteps, can be seen in Figure 12. From the figure it is clear that a static wavefront is formed which moves throughout space at a constant speed. This wavefront does not hold at the boundaries in order to satisfy the conditions imposed there. As a side note, the solutions did exhibit monotonicity issues. After discussion with Simpson, it was determined that this is due to MATLAB's pdepe function using the method of lines,

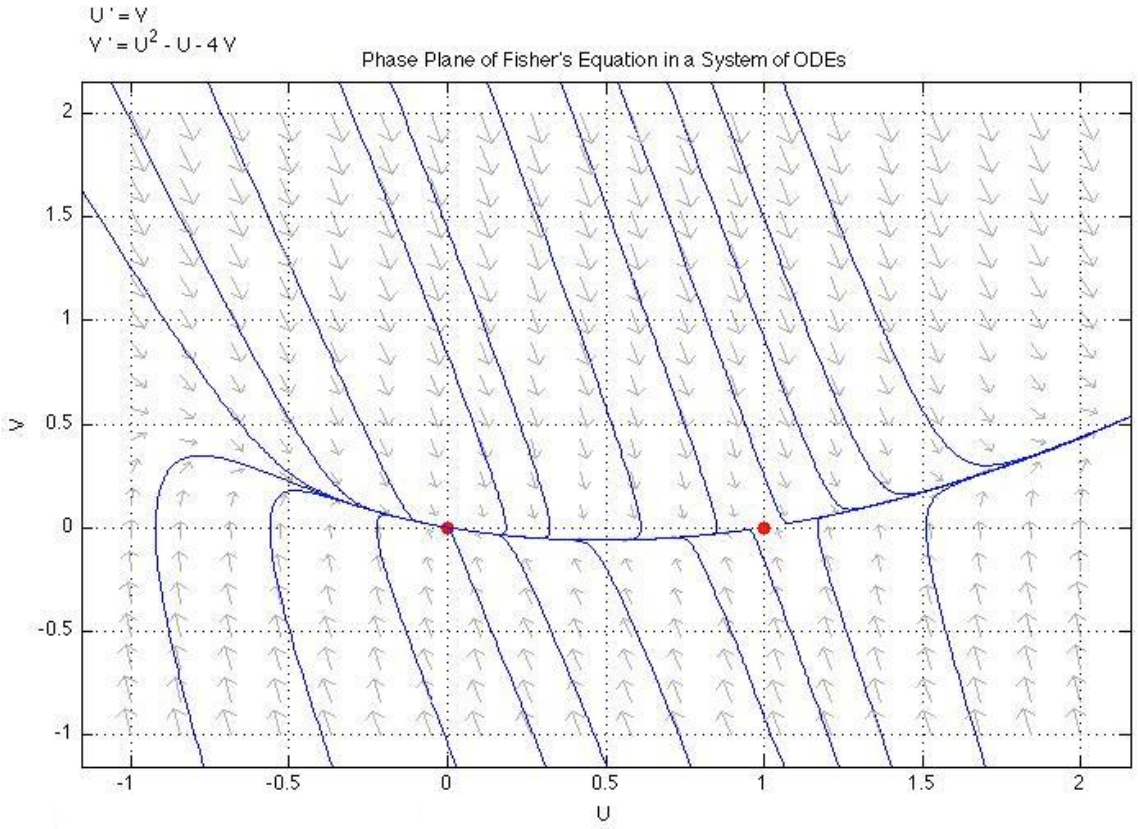

Figure 11: Phase plane of the system of ODEs that describe the travelling wave solutions to Fisher's equation, where $C = 4$. The red dots are the critical points and the blue lines are the phase trajectories. At $(0, 0)$ there is a stable node and at $(1, 0)$ there is a saddle point.

which can result in physically unrealistic solutions. It was decided that alternative means for solving Fisher's equation would be pursued as a result.

Solutions to Fisher's equation were investigated for various initial conditions to observe how the logistic source term reacts to overpopulated and underpopulated regions. As expected, provided $U \geq 0$, the solutions continue to form a travelling wavefront. This is due to the logistic source term compensating for regions which do not satisfy the carrying capacity of unity. Likewise, in the event that $U < 0$, the solutions diverge to $-\infty$. It is clear that the logistic source term plays an integral role in forming travelling wave solutions of a specific amplitude.

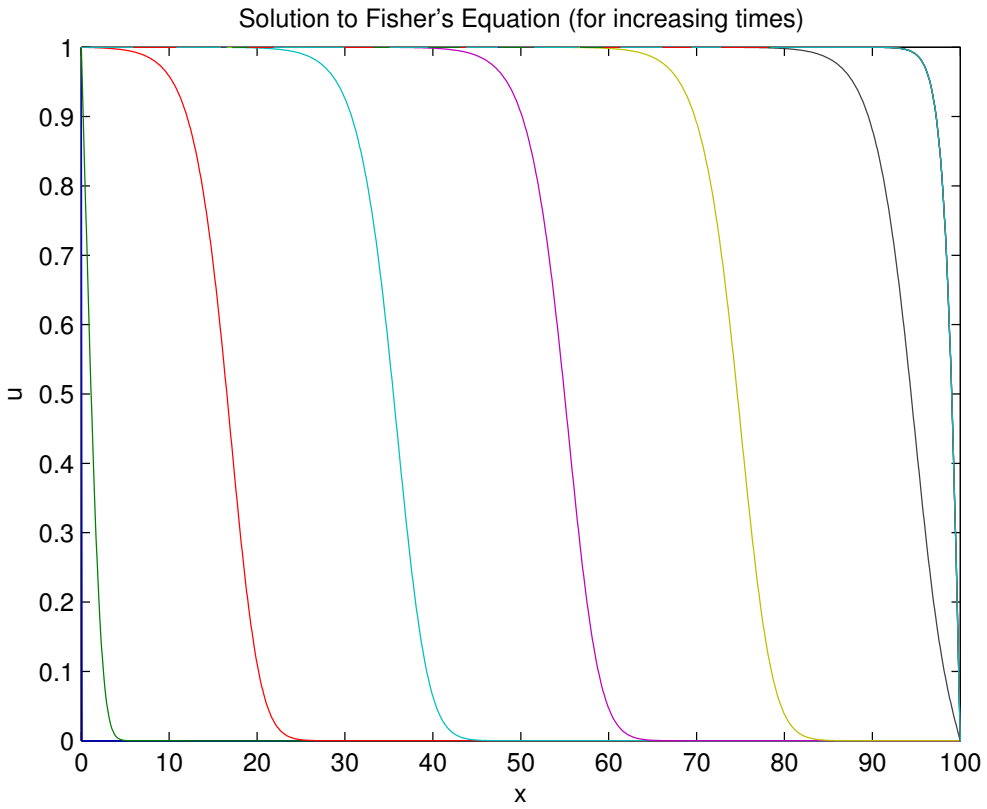

Figure 12: Travelling wave solutions to Fisher's equation for increasing times. The following boundary conditions are applied: $U(0,t) = 1$ and $U(100,t) = 0$, hence there are steep wave fronts at the boundaries.

References

[1] José Canosa. "On a nonlinear diffusion equation describing population growth". In: *IBM Journal of Research and Development* 17.4 (1973), pp. 307–313.

[2] *Periodic Boundary Conditions*. Virtual Institute of Nano Films. 2012. URL: http://www.mbnexplorer.com/users-guide/6-numerical-methods-interatomic-interactions/63-boundary-conditions/632-periodic.

[3] Michael J Plank and Matthew J Simpson. "Lattice-Free Models of Cell Invasion: Discrete Simulations and Travelling Waves". In: *Bulletin of mathematical biology* 75.11 (2013), pp. 2150–2166.

[4] John C Polking. *ODE Software for MATLAB*. Rice University. Apr. 2002. URL: http://math.rice.edu/~dfield/.

[5] *Reflective Boundary Conditions*. Virtual Institute of Nano Films. 2012. URL: http://www.mbnexplorer.com/users-guide/6-numerical-methods-interatomic-interactions/63-boundary-conditions/631-reflective.

[6] John Renze and Eric W Weisstein. *Law of Large Numbers*. MathWorld–A Wolfram Web Resource. URL: http://mathworld.wolfram.com/LawofLargeNumbers.html.

[7] Matthew J Simpson, Kerry A Landman, and Barry D Hughes. "Cell invasion with proliferation mechanisms motivated by time-lapse data". In: *Physica A: Statistical Mechanics and its Applications* 389.18 (2010), pp. 3779–3790.

[8] Matthew Simpson, K Landman, and B Hughes. "Diffusing populations: ghosts or folks". In: *Australasian Journal of Engineering Education* 15.2 (2009), pp. 59–68.